Smart management of integrated energy systems through co-optimization with long and short horizons

Smart management of integrated energy systems through co-optimization with long and short horizons

Costanza Saletti[a*], Mirko Morini[a,b], Agostino Gambarotta[a,b]

[a] *Center for Energy and Environment (CIDEA), University of Parma, Parco Area delle Scienze 181/A, 43124 Parma, Italy*
[b] *Department of Engineering and Architecture, University of Parma, Parco Area delle Scienze 181/A, 43124 Parma, Italy*

* Corresponding author: costanza.saletti@unipr.it

Abstract

The integration of all sectors of energy production, distribution and consumption in multi-source energy networks has lately gained attention as an attractive strategy to deal with the challenges raised by decarbonization roadmaps. For such a network to become a smart energy system, however, it needs to be managed and controlled in a smart way. While existing techniques mainly focus either on short-term unit commitment or on yearly scheduling separately, this work presents an original combined optimization algorithm which merges the two methods, in order to enhance system real-time control with long-term evaluations (e.g. incentives and yearly constraints). The control architecture comprises three coordinated optimization levels, each periodically updated through the receding time horizon strategy. A long-term supervisory module performs whole-year optimal scheduling accounting for long-term factors and determines the constraints for a short-term supervisory module which, in turn, optimizes the control action for the energy production system in real-time. In parallel, energy distribution modules minimize energy supply to the different portions of the distribution network downstream. Simulation results on a hospital case study demonstrate a 9.7% reduction in total operating cost over the whole year, as well as an increase in revenues deriving from incentives for high efficiency cogeneration.

Keywords: Multi-energy systems; Model Predictive Control; long-term optimization; short-term optimization; District Heating and Cooling Networks; Combined Heat and Power plant

1. Introduction

The transition toward clean energy, aiming to reduce energy-related carbon emissions and mitigate the impact of climate change on the environment, is gradually phasing out fossil fuels in favor of a higher penetration of renewable-based energy production technologies. Such a transformation of the global energy sector toward decarbonization is giving rise to systems of increased complexity as well as to new challenges in system management, due to the non-programmable character of solar and wind renewables [1]. A change of paradigm in which flexible demand adapts to variable generation rather than the opposite is expected to be led by sector integration [2]. This encompasses the interconnection, interaction and integration of all sectors of energy production, distribution and consumption (i.e. heating, cooling, electricity, and gas), in order to exploit the synergies arising among them [3].

According to Mancarella [4], these multi-energy systems include different interacting energy vectors and coupling devices and are seen with a whole-system approach. It is stated that their technical, economic and environmental benefits are significant compared to the individual systems taken separately. The integrated energy infrastructure as defined by Guelpa et al. [5] comprises energy conversion units (e.g. boilers as gas-to-heat, cogeneration plants as gas-to-heat and power, and electrolyzers as power-to-gas), the networks used for the energy vector distribution (e.g. gas, power, district heating and cooling), energy storage devices (e.g. tanks for heat, cold or fuel, and electrical batteries) and finally the end-users. This framework enables (i) higher flexibility and reliability thanks to the multiple degrees of freedom, (ii) reduced waste of resources due to the possibility to switch between energy vectors when regarded as more cost effective according to the boundary conditions, and (iii) a more rational exploitation of renewables and waste heat.

Nonetheless, several barriers to the realization of higher efficiency and flexibility of integrated systems can be identified [6], related in particular to their operation. All components of such complex systems should be coordinated in an optimal way through suitable optimization algorithms, in order to deliver the best performance while meeting system constraints. More importantly, the potential of

multi-energy infrastructures can be fully unlocked through smart control systems which autonomously optimize and update the management strategy in real-time [7], depending on the availability of the renewable energies [8], network state and consumer demands. Indeed, the introduction of a smart management strategy allows, in practice, the transition from a multi-energy system to a *smart energy system* [9,10].

The currently available methods for optimizing the operation and management of multi-source district energy network can be divided into short-term and long-term algorithms.

On the one hand, the former type distributes the generation of different forms of energy among the available conversion devices over a time horizon that spans from a few hours up to one week, by considering the day-ahead forecast of end-user energy demands. This is a widely investigated problem also known as Unit Commitment [11], which has to be extended to different energy vectors when multi-energy systems are considered. In most works, this problem is solved through Mixed Integer Linear Programming (MILP) and is applied to case studies with different purposes and features: operation planning of combined cooling, heating and power systems [12], robust optimization of microgrids [13], temperature optimization of a 5^{th} generation District Heating and Cooling (DHC) network [14]. Moreover, in order to investigate demand side management potential, Ghilardi et al. [15] also include the thermal energy balance of buildings connected to the multi-energy system in the MILP formulation, while Capone et al. [16] propose a bi-level optimization structure with the addition of a genetic algorithm. In other cases, the load allocation can be defined through different algorithms, such as Dynamic Programming [17].

MILP methods display the great advantage of ensuring global optimality, but are subject to several limitations, as reviewed by Urbanucci [18]. In particular, the dimension of the problem can be kept computationally feasible, due to the short time horizons, and therefore it can be applied for real-time controllers. However, a growing number of energy conversion plants and end-users, which is typical of district energy applications, entails a substantial increase in the number of control variables and, consequently, in the required computational effort [19]. Despite this challenging issue, a few papers

in the literature use such short-term optimization algorithms in district energy control applications [20]. For instance, Mugnini et al. [21] present a control method based on Model Predictive Control (MPC) for a multi-energy system integrated within an individual building with specific focus on assessing the flexibility potential of the building during the cooling season. Further studies are necessary to extend the results in terms of cost and primary energy reduction at district level. Banta et al. [22] present an advanced MPC paradigm for a campus-size microgrid. Moser et al., instead, develop a modular MILP energy management system for urban networks which can repeatedly update its optimization according to the MPC concept, and test its performance in present and future simulation scenarios [23]. It is worth noting, however, that MPC is currently more widespread in the investigation of microgrids [24] or heat-pump systems [25], compared to smart energy systems in general.

On the other hand, long-term algorithms dispatch the energy production for one or multiple years with an hourly or daily resolution. The whole-year horizon allows long-term features to be considered, such as seasonal storage [26]. The most part of research on the long-term optimization of district energy networks primarily aims at system design, scenario investigation and yearly operation scheduling. There is generally no focus on real-time control, due to the scale of the problem and consequent great computational effort required. Gabrielli et al. [27] provide optimal design guidelines for multi-energy systems with seasonal storage when there is uncertainty on forecasted data. This is achieved by aggregating yearly time series on a minimum number of typical design days, in order to reduce the number of variables and keep the computational costs down. While the approach of using representative days is widely used [28,29], other works reduce the computational demand of whole-year energy scheduling with hourly resolution by using a sliding month approach [30] or a rolling horizon weekly strategy [31].

Recent research is heading toward not only the optimal integration of different energy vectors, as outlined so far, but also the integration of different time scales and stages [32]. This means that optimization algorithms with different time features (i.e. time horizon and granularity) are combined

in a hierarchical [33] or concurrent fashion, in order to decompose the problem into simpler sub-problems and fulfill multiple goals. Bornand et al. [34] demonstrate a multi-period formulation to generate long-term investment planning scenarios for large heterogeneous district energy consumers, such as hospitals, airports and educational complexes. The proposed methodology couples energy integration techniques with multi-objective optimization to determine the optimal size of alternative energy equipment in a long-term perspective. However, the analysis does not take system operation and control into account. Naughton et al. [35] investigate the market participation of an electricity-hydrogen power plant through a three-stage optimization framework, where the three optimization problems perform device scheduling daily, preliminary power plant dispatch every 30 minutes and actual dispatch every 5 minutes, respectively [36]. A multi-time-space scale collaborative model for coordinating multiple energy communities is established by Li et al. [37], who integrated optimization levels ranging from real-time adjustment to day-ahead scheduling.

As summarized in Table 1, the overview of existing research on the optimization of multi-energy systems shows that, in general, short-term and long-term algorithms cover different objectives and show conflicting advantages and limitations. It is clear that short-term optimal operation is able to include only immediate goals such as operating cost and energy consumption and, as such, it has no potential in including yearly objectives and features. For instance, the Italian regulation on high efficiency cogeneration establishes that high efficiency credits (namely white certificates) are awarded to systems that meet two energy saving criteria evaluated on a yearly basis or with reference to a given period [31]. Similar indicators can be found in other European or country-specific policies. Therefore, a short-term control algorithm certainly leads to immediate smarter operation, but it may also move the system away from achieving long-term benefits. In parallel, long-term optimization may be able to determine a profitable maintenance scheduling, but this cannot be reflected in a smarter control. Furthermore, the latter is not able to deal rapidly and effectively with external events that would require reassessing long-term system planning. These examples show that great potential lies in the combination of different time perspectives in the optimal control of energy systems.

Table 1. Features of short- and long-term optimization algorithms for multi-energy systems.

	Short-term algorithms	Long-term algorithms
Objectives and constraints	Operating cost Energy consumption Indoor comfort Operating constraints	Yearly operating cost Yearly energy consumption Energy efficiency incentives Maintenance schedule Investment costs
Advantages	Low computational cost Suitable for control Plant operation included	Long-term goals and constraints included
Disadvantages	Only short-term goals and constraints Not optimal with regard to yearly features	High computational cost Not suitable for control Typical operating days must be used

To the best of the authors' knowledge, the literature lacks real-time control methods that are able to merge the advantages of both types of algorithms, and thus to optimize the operation of district energy systems with the simultaneous inclusion of yearly objectives.

This work aims to bridge the gap between the two approaches by presenting a combined optimization algorithm for both *sector integration* and *time integration* of multi-source district energy systems. The approach is based on multi-agent hierarchical Model Predictive Control formulation with multiple space and time layers, in order to merge long- and short-term optimization goals and constraints. The long-term MPC layer performs yearly scheduling and calculates long-term constraints to be sent to the short-term MPC layer which, in turn, operates real-time system control. The two problems are solved individually with their specific variables, constraints and cost function, but the constant communication between them allows the limitations of each layer to be compensated. This global strategy combines the benefits of both types of optimization algorithm and paves the way toward multi-period system optimality of integrated energy networks regardless of their specific configuration. The control verification is carried out on a large hospital site by means of whole-year simulations in actual control configuration.

2. Methods and control architecture

This section describes the novel combined optimization algorithm for optimally managing integrated energy networks with multiple interacting energy vectors and required energy services, as well as several energy conversion plants to be coordinated in the thermal power station.

The main objectives and features of the algorithms are as follows:

- Inclusion of all sections of the system, ranging from the thermal power station to the distribution network and end-users' substations.
- Modular extension to different system configurations, with particular reference to small-scale district energy, e.g. campus, hospitals, and small neighborhoods.
- Fulfillment of end-user demand of all energy vectors (e.g. heating, cooling, electricity, and steam) with the lowest operating cost on a yearly basis, including the revenues deriving from incentives.
- Coupling of two communicating optimization layers which operate at two different time scales, i.e. long-term optimization coupled with short-term optimization.
- Application in a real-time controller based on MPC.

One of the most notable characteristics of MPC is the receding time horizon strategy [38]. In practice, MPC calculates an open-loop sequence of optimal control actions for a time-discrete prediction horizon in the future, and applies the first element of this sequence. After a time-step, the actual system behavior is monitored, the prediction horizon is moved forward, and the updated optimal control sequence is recalculated starting from new system knowledge. This continuous procedure improves the control robustness with regard to disturbances and unpredictable events, but it also requires an optimization algorithm that computes the solution significantly faster than system dynamics. As far as multi-energy systems are concerned, most existing optimization algorithms are not suitable for MPC since they do not meet this requirement. Conversely, the combined algorithm proposed in this work is developed with special focus on real-time control applicability. The details on the original control architecture and all its layers are reported in the following sections.

2.1 Control algorithm architecture

A generic district energy system can be divided into the district heating and cooling network, comprising several distribution loops and end-users, and the thermal power station, which aggregates all energy conversion plants. Performing optimal control of the whole system at the same time with a small time resolution and a yearly perspective would be infeasible, if tackled by a single traditional algorithm. In this work, this task is executed in a modular and manageable way by dividing the problem into smaller hierarchical sub-problems.

As illustrated in Figure 1, the proposed control architecture combines three interacting space and time control layers:

- **Distribution modules**. Each of these parallel modules is an autonomous MPC agent that manages energy distribution to a section of the heating and cooling network (e.g. branch supplying a building) and forecasts its heating and cooling requirements over a short-term prediction horizon (e.g. the following two days).
- **Short-Term Supervisory module**, namely **ShoTS**. It is a low-level supervisory MPC agent which controls the thermal power station in real time, based on a short-term objective and prediction horizon. This layer receives (i) the demand forecast from the distribution modules, (ii) long-term constraints calculated by a high-level supervisory controller, and (iii) feedback on the actual operation of the system.
- **Long-Term Supervisory module**, namely **LoTS**. It is a high-level supervisory controller that (i) receives the actual system operation in the form of the cumulated energy and fuel consumed, (ii) solves the yearly scheduling problem of the thermal power station with a daily time resolution, thus including long-term factors, and (iii) generates the long-term constraints for ShoTS.

In the long run, real-time automatic control carried out by ShoTS should lead to the fulfillment of the yearly goals, since it is forced to follow indications given by LoTS. Moreover, in agreement with the receding time horizon strategy typical of MPC, the optimization problems of each module are updated

and solved at every related time-step, i.e. 15 minutes for the distribution and ShoTS, and one day for LoTS. The other main features are summarized in Table 2.

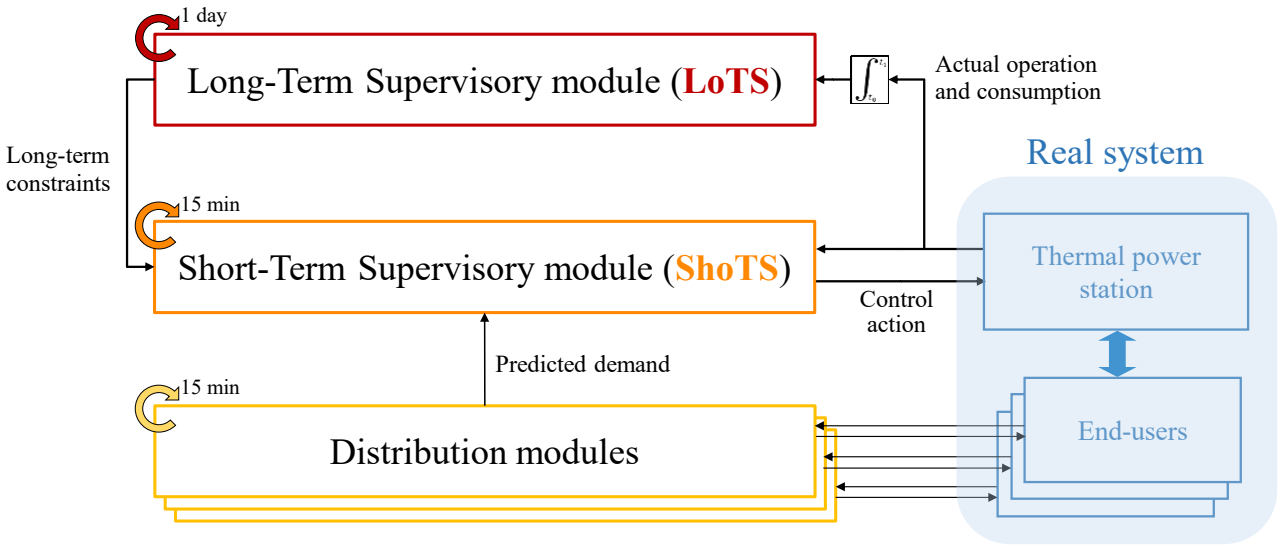

Figure 1. Three-layer MPC control architecture for district energy networks.

Table 2. Features of the three modules of the combined optimization algorithm.

	Distribution module	ShoTS module	LoTS module
Objective function	Minimize energy supplied to end-user	Minimize operating cost	Minimize yearly cost
Constraints	End-user indoor comfort temperature	Meet energy demand, plant operation, long-term constraints	Meet daily demand, efficiency incentives, contracts and maintenance
Disturbances	Outdoor temperature, occupation schedule	Energy demand, hourly cost of electricity	Energy demand, daily cost of electricity
Prediction horizon	2 days	2 days	Whole year
Time-step	15 minutes	15 minutes	1 day
Algorithm	Dynamic Programming	Mixed Integer Linear Programming	Linear Programming

2.2 Long-term Supervisory module

The LoTS module schedules the energy produced every day by the plants in the thermal power station in order to match the daily energy demand of all energy vectors. The module receives the forecast of the daily energy demand and average outdoor temperature for the remaining part of the year, as well as the daily average market price of electricity.

2.2.1 Optimization variables

Each energy conversion unit receives an energy vector as input (e.g. fuel for a cogeneration unit) and returns one or more energy vectors as output (e.g. electricity and heat for the same unit). In the remainder of the manuscript, the superscripts *h*, *c*, *el* and *f* represent heating, cooling, electricity and fuel energy, respectively, while the subscripts *in* and *out* indicate input and output energy of a given unit, respectively. For instance, heat-only boilers are characterized by E^{f}_{in} and E^{h}_{out}, while cogeneration plants by E^{f}_{in}, E^{h}_{out} and E^{el}_{out}. In this module, the units are modeled with input-output relationships characterized by a fixed nominal efficiency η^{i} from energy vector *l* to energy vector *i*, as written in Eq. (1) for a generic unit *j*:

$$E^{i}_{out,j} = \eta^{i}_{j} E^{l}_{in,j} \quad (1)$$

With this notation, the optimization variables for each day *k* of the LoTS problem are:

1. $E^{l}_{in,j,k}$: daily input energy of form *l* to unit *j*;
2. $E_{diss,j,k}$: daily heat dissipated from unit *j*;
3. $E_{gb,k}$: daily electrical energy bought from the power grid;
4. $E_{gs,k}$: daily electrical energy sold to the power grid;
5. $\varepsilon_{j,k}$: daily availability of unit *j* due to maintenance or constraints on operating hours, comprised in the interval [0,1].

In order to determine the long-term constraints for ShoTS, maximum and minimum auxiliary variables are added for daily input energy and exchange with the power grid:

6. $M_{j,k}$: maximum daily input energy to unit *j* (or exchange with grid);
7. $m_{j,k}$: minimum daily input energy to unit *j* (or exchange with grid).

The concept is qualitatively illustrated in Figure 2: the variables *M* and *m* bind the actual input energy and determine an optimal band of operation that shall be met for the remaining part of the year. The first section of these optimal bands, corresponding to the number of days of the ShoTS prediction horizon, is used as a long-term constraint to further bind the ShoTS problem and push it toward a solution that also meets the LoTS yearly goals.

If seasonal storage is present, there are additional variables for its state of charge, daily charge and discharge energy, and proper constraints. In this research, the seasonal storage implementation is omitted for the sake of brevity, but can be added with no effort following, for instance, the approach in [39].

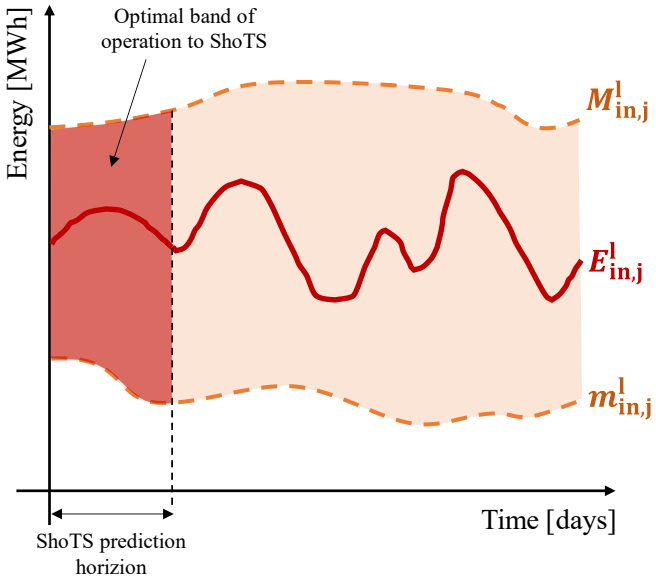

Figure 2. Qualitative representation of the optimal band of operation as long-term constraints determined by the maximum and minimum auxiliary variables in the LoTS problem.

2.2.2 Objective function

If the problem is written for a N_d number of days until the end of the calendar year, the objective function is the total operating cost for the given period, including cost of fuel, electricity and incentives obtained, for instance, due to high efficiency cogeneration:

$$\sum_{k=1}^{N_d}\left[\frac{c_f}{LHV}\sum_j E^f_{in,j,k} + C_{gb,k}E_{gb,k} - C_{gs,k}E_{gs,k}\right] - \sum_j C_{inc,j} \quad (2)$$

where c_f is the fuel cost, C_{gb} and C_{gs} are the average daily purchase and sale costs of electricity. The second sum includes the revenues from incentives. In particular, the Italian legislation rewards a high efficiency cogeneration unit with energy efficiency certificates proportional to the primary energy saving [31].

2.2.3 Constraints

The constraints of meeting the daily demand of energy vector *l* (i.e. $E^{l}_{dem,k}$) for each day *k* is given by Eqs. (3). The electricity version Eq. (3c) accounts for grid exchange while the heat version Eq. (3a) subtracts the dissipated heat.

$$\sum_{j} E^{h}_{out,j,k} - \sum_{j} E_{diss,j,k} - \sum_{j} E^{h}_{in,j,k} = E^{h}_{dem,k} \quad \forall\, k \tag{3a}$$

$$\sum_{j} E^{c}_{out,j,k} - \sum_{j} E^{c}_{in,j,k} = E^{c}_{dem,k} \quad \forall\, k \tag{3b}$$

$$\sum_{j} E^{el}_{out,j,k} - \sum_{j} E^{el}_{in,j,k} + E_{gb,k} - E_{gs,k} = E^{el}_{dem,k} \quad \forall\, k \tag{3c}$$

The constraints for the maximum and minimum auxiliary variables are:

$$m_{in,j,k} \le E_{in,j,k} \le M_{in,j,k} \quad \forall\, j, \forall\, k \tag{4a}$$

$$m_{gb,k} \le E_{gb,k} \le M_{gb,k} \quad \forall\, k \tag{4b}$$

$$m_{gs,k} \le E_{gs,k} \le M_{gs,k} \quad \forall\, k \tag{4c}$$

The technical and operating constraints are:

$$M_{in,j,k} \le \varepsilon_{j,k} E_{in,max,j} \quad \forall\, j, \forall\, k \tag{5}$$

$$E_{diss,j,k} \le E^{h}_{out,j,k} \quad \forall\, j, \forall\, k \tag{6}$$

where $E_{in,max,j}$ is a parameter characteristic of each unit *j*, representing its maximum input energy in a day at full load. In addition, when there is a scheduled maintenance period for a given unit, the upper boundary of the corresponding ε is set to 0.

The year-based constraints involve, for example, the yearly maximum and minimum fuel purchase established in the supply contract (i.e. $E^{f}_{max,y}$ and $E^{f}_{min,y}$, respectively) in Eqs. (7):

$$\sum_{k=1}^{N_d} \sum_{j} m^{f}_{in,j,k} \ge E^{f}_{min,y} - E^{f}_{past} \tag{7a}$$

$$\sum_{k=1}^{N_d} \sum_{j} M^{f}_{in,j,k} \le E^{f}_{max,y} - E^{f}_{past} \tag{7b}$$

where E^{f}_{past} is the fuel energy actually consumed by the real system in the previous period of the year, obtained by monitoring and cumulating its actual past operation. The same set of equations with

corresponding past cumulated parameters (indicated by the subscript *past*) can be written for electricity bought and sold to the grid, or for other energy vectors.

According to the Italian regulation, the constraints a cogeneration unit *j* should fulfil to obtain the high efficiency cogeneration label are specific reference boundaries on overall efficiency ($\eta^{\mathrm{I}}_{\mathrm{ref}}$) and Primary Energy Saving ($\mathrm{PES}_{\mathrm{ref}}$):

$$\eta_{\mathrm{j}}^{I} = \frac{\sum_{k=1}^{N_{\mathrm{d}}} m_{\mathrm{out,j,k}}^{\mathrm{el}} + E_{\mathrm{past,j}}^{\mathrm{el}} + \sum_{k=1}^{N_{\mathrm{d}}} \left(m_{\mathrm{out,j,k}}^{\mathrm{h}} - E_{\mathrm{diss,j,k}}\right) + E_{\mathrm{past,j}}^{\mathrm{h}}}{\sum_{k=1}^{N_{\mathrm{d}}} m_{\mathrm{in,j,k}}^{\mathrm{f}} + E_{\mathrm{past,j}}^{\mathrm{f}}} \geq \eta_{\mathrm{ref}}^{I} \tag{8a}$$

$$\mathrm{PES_j} = 1 - \left[\frac{\sum_{k=1}^{N_{\mathrm{d}}} m_{\mathrm{out,j,k}}^{\mathrm{el}} + E_{\mathrm{past,j}}^{\mathrm{el}}}{\left(\sum_{k=1}^{N_{\mathrm{d}}} m_{\mathrm{in,j,k}}^{\mathrm{f}} + E_{\mathrm{past,j}}^{\mathrm{f}}\right)\eta_{\mathrm{el,ref,j}}\, p_{\mathrm{j}}} + \frac{\sum_{k=1}^{N_{\mathrm{d}}} \left(m_{\mathrm{out,j,k}}^{\mathrm{h}} - E_{\mathrm{diss,j,k}}\right) + E_{\mathrm{past,j}}^{\mathrm{h}}}{\left(\sum_{k=1}^{N_{\mathrm{d}}} m_{\mathrm{in,j,k}}^{\mathrm{f}} + E_{\mathrm{past,j}}^{\mathrm{f}}\right)\eta_{\mathrm{h,ref,j}}}\right]^{-1} \geq \mathrm{PES_{ref}} \tag{8b}$$

where $\eta_{\mathrm{el,ref}}$ and $\eta_{\mathrm{h,ref}}$ are reference electrical and thermal efficiency when electricity and heat are produced individually, and *p* is a grid loss penalty.

Finally, there are constraints on maximum operating hours OH_{max}:

$$\sum_{k=1}^{N_{\mathrm{d}}} \varepsilon_{\mathrm{j,k}} \leq \frac{OH_{\mathrm{max,j}} - OH_{\mathrm{past,j}}}{24} \quad \forall\, j \tag{9}$$

Moreover, other custom equations can be easily inserted if additional limitations are present.

Since all variables are continuous and all constraints and the cost function are linear (Eqs. (8) can be easily reformulated in linear form), LoTS is a Linear Programming problem.

2.3 Short-term Supervisory module

The ShoTS module contains a customized version of a highly detailed unit commitment problem which is further bound with the long-term constraints described previously. It receives the forecast of the demand, outdoor temperature and market price of electricity for the future prediction horizon. The goal is to define the operation of all conversion units in the thermal power station to minimize a given criterion. The deriving problem is an MILP due to the presence of continuous and binary variables.

2.3.1 Optimization variables

Following the notation used in Section 2.2, the optimization variables for each time-step k of the ShoTS problem are:

1. $P^{l}_{in,j,k}$: input power of form l to unit j;
2. $\delta_{j,k}$: on-off switch of unit j, binary variable that is 1 if the unit is producing and 0 otherwise;
3. $\gamma_{j,k}$: stand-by switch of unit j, binary variable that is 1 if the unit is kept in stand-by mode (i.e. on but not producing) and 0 otherwise;
4. $SU^{l}_{j,k}$: start-up cost as additional input power of form l for start-up of unit j;
5. $P_{diss,j,k}$: thermal power dissipated from unit j;
6. $P_{gb,k}$: electrical power bought from the grid;
7. $P_{gs,k}$: electrical power sold to the grid.

Compared to LoTS, the conversion units are modeled with a more detailed relationship which takes into account the efficiency reduction at partial load. The linearity of the problem is paramount to keep the computational cost down. Hence, the input-output performance curve of each unit j is linearized as in Eq. (10) with performance coefficients α and β, or it is transformed into a piece-wise linear function [40].

$$P^{i}_{out,j} = \alpha^{i}_{j} E^{l}_{in,j} + \beta^{i}_{j} \delta_{j} \quad (10)$$

In similarity with the LoTS module, if any kind of short-term storage is present, the additional variables for the state of charge, charge and discharge power, and the related constraints can be easily added. Here, this part is omitted without losing the generality of the approach.

2.3.2 Objective function

Given Δt is the amplitude of a time-step and N the number of time-steps of the ShoTS prediction horizon, corresponding to D days, the objective function Eq. (11) is the total operating cost for this time interval:

$$\sum_{k=1}^{N}\left[\frac{c_{\mathrm{f}}}{LHV}\sum_{\mathrm{j}}\left(P_{\mathrm{in,j,k}}^{\mathrm{f}}+SU_{\mathrm{j,k}}^{\mathrm{f}}+\gamma_{\mathrm{j,k}}P_{\mathrm{sby,j}}^{\mathrm{f}}\right)+c_{\mathrm{gb,k}}P_{\mathrm{gb,k}}-c_{\mathrm{gs,k}}P_{\mathrm{gs,k}}\right]\Delta t \tag{11}$$

where c_{gb} and c_{gs} are the hourly purchase and sale costs of electricity and $P^{\mathrm{f}}{}_{\mathrm{sby,j}}$ is the additional fuel power necessary for maintaining unit *j* in stand-by mode.

2.3.3 Constraints

Given $P^{\mathrm{l}}{}_{\mathrm{dem,k}}$ is the power demand of vector l at time-step k, this is met through constraints similar to Eqs. (3):

$$\sum_{\mathrm{j}}\left(P_{\mathrm{out,j,k}}^{\mathrm{h}}-P_{\mathrm{diss,j,k}}\right)-\sum_{\mathrm{j}}\left(P_{\mathrm{in,j,k}}^{\mathrm{h}}+SU_{\mathrm{j,k}}^{\mathrm{h}}+\gamma_{\mathrm{j,k}}P_{\mathrm{sby,j}}^{\mathrm{h}}\right)=P_{\mathrm{dem,k}}^{\mathrm{h}}\quad\forall\,k \tag{12a}$$

$$\sum_{\mathrm{j}}P_{\mathrm{out,j,k}}^{\mathrm{c}}-\sum_{\mathrm{j}}P_{\mathrm{in,j,k}}^{\mathrm{c}}=P_{\mathrm{dem,k}}^{\mathrm{c}}\quad\forall\,k \tag{12b}$$

$$\sum_{\mathrm{j}}P_{\mathrm{out,j,k}}^{\mathrm{el}}-\sum_{\mathrm{j}}\left(P_{\mathrm{in,j,k}}^{\mathrm{el}}+SU_{\mathrm{j,k}}^{\mathrm{el}}+\gamma_{\mathrm{j,k}}P_{\mathrm{sby,j}}^{\mathrm{el}}\right)+P_{\mathrm{gb,k}}-P_{\mathrm{gs,k}}=P_{\mathrm{dem,k}}^{\mathrm{el}}\quad\forall\,k \tag{12c}$$

The technical and operating constraints include upper and lower power exchange boundaries in Eqs. (13), up and down ramp constraints in Eq. (14), start-up costs in Eq. (15), as well as the inequality for heat dissipation in Eq. (16):

$$\delta_{\mathrm{j,k}}P_{\mathrm{in,min,j}}\leq P_{\mathrm{in,j,k}}\leq\delta_{\mathrm{j,k}}P_{\mathrm{in,max,j}}\quad\forall\,j,\forall\,k \tag{13a}$$

$$0\leq P_{\mathrm{gb,k}}\leq P_{\mathrm{gb,max}}\quad\forall\,k \tag{13b}$$

$$0\leq P_{\mathrm{gs,k}}\leq P_{\mathrm{gs,max}}\quad\forall\,k \tag{13c}$$

$$\Delta P_{\mathrm{down,j}}\leq P_{\mathrm{in,j,k+1}}-P_{\mathrm{in,j,k}}\leq\Delta P_{\mathrm{up,j}}\quad\forall\,j,\forall\,k\,\epsilon\,[1,N) \tag{14}$$

$$P_{\mathrm{SU,j}}^{\mathrm{l}}\left(\delta_{\mathrm{j,k+1}}-\delta_{\mathrm{j,k}}-\gamma_{\mathrm{j,k}}\right)-SU_{\mathrm{j,k}}^{\mathrm{l}}\quad\forall\,j,\forall\,k\,\epsilon\,[1,N) \tag{15a}$$

$$\delta_{\mathrm{j,k}}+\gamma_{\mathrm{j,k}}\leq 1\quad\forall\,j,\forall\,k \tag{15b}$$

$$\gamma_{\mathrm{j,k+1}}-\gamma_{\mathrm{j,k}}-\delta_{\mathrm{j,k}}\leq 0\quad\forall\,j,\forall\,k\,\epsilon\,[1,N) \tag{15c}$$

$$P_{\mathrm{diss,j,k}}\leq P_{\mathrm{out,j,k}}^{\mathrm{h}}\quad\forall\,j,\forall\,k \tag{16}$$

In the equations above, ΔP_{up} and ΔP_{down} are ramp boundaries when increasing or decreasing the power input to a unit, respectively, while $P^{\mathrm{l}}{}_{\mathrm{SU,j}}$ is a fixed additional input power when unit *j* is subject to a start-up. Eqs. (15) together indicate that a unit cannot be switched on and in stand-by mode at the same time, and this additional input power is assigned only when there is actually a start-up. The initial values of δ and γ are set starting from the actual plant state acquired from the real system.

Other constraints regard the unit operation minimum up-time and down-time, which follow the method presented in [40] and are omitted for the sake of brevity. Furthermore, proper hierarchical inequality constraints [41] are added in order to avoid the symmetry problem that appears in MILP when there are multiple identical conversion units.

Finally, the long-term constraints are formulated starting from the solution of the LoTS problem. Two examples of the maximum and minimum fuel consumption over the ShoTS prediction horizon and maximum operating time of unit *j* are reported in Eqs. (17) and (18), respectively. Nevertheless, analogous formulations can be written for other requirements, such as the maximum and minimum production of a cogeneration unit or electricity exchange with the grid.

$$\sum_{k=1}^{D}\sum_{\mathrm{j}} m^{\mathrm{f}}_{\mathrm{in,j,k}} \leq \sum_{k=1}^{N}\sum_{\mathrm{j}} P^{\mathrm{f}}_{\mathrm{in,j,k}}\,\Delta t \leq \sum_{k=1}^{D} M^{\mathrm{f}}_{\mathrm{in,j,k}} \tag{17}$$

$$\sum_{k=1}^{N} \delta_{\mathrm{j,k}}\,\Delta t \leq \sum_{k=1}^{D} \varepsilon_{\mathrm{j,k}} \cdot 3600 \cdot 24 \quad \forall\, j \tag{18}$$

where *m*, *M* and ε are obviously related to the LoTS optimal solution.

2.4 Distribution module

The development and demonstration of the distribution module through simulation and real-world case studies can be found in [38,42]. It contains a simplified gray-box model of the building, which can be identified with experimental or simulation datasets of a few days [38], and of the related branch of the district heating and cooling network. The model state is the indoor temperature, which is bound between the comfort limits when the building is occupied. Underlying physical phenomena such as heat losses and time delays in heat distribution are considered. An original Dynamic Programming algorithm regulates the network water mass flow rate and supply temperature to minimize the heating or cooling energy transferred through the branch over a two-day prediction horizon, while making sure that user comfort is maintained.

This approach has previously led to a significant reduction in energy consumption as regards the distribution side. This research extends its application by linking it to the combined ShoTS-LoTS algorithm with two time scales.

2.5 Communication between modules

The general logic of the proposed control solution and the communication between the algorithm and the external elements is represented in the flowchart in Figure 3.

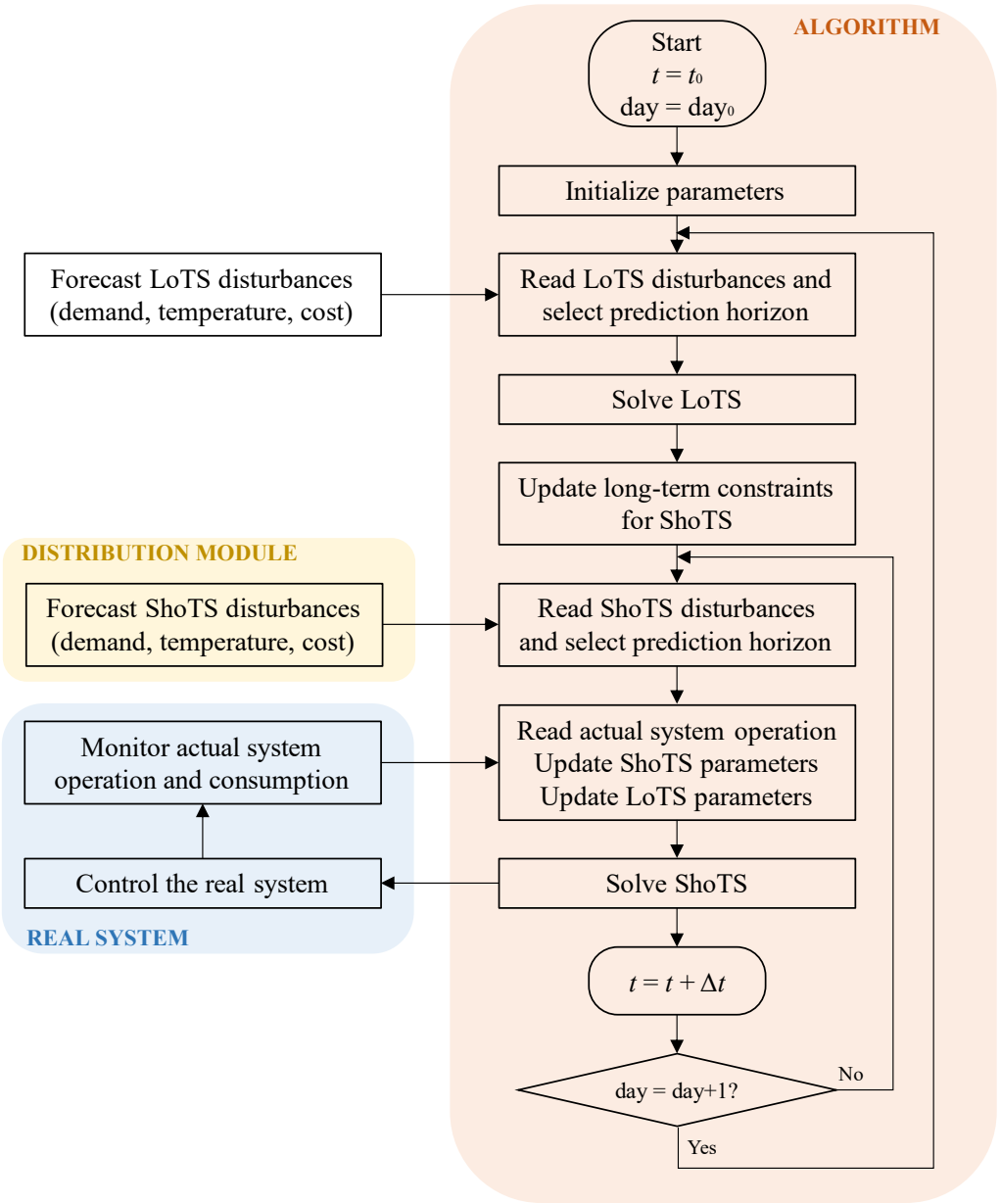

Figure 3. Flowchart of the communication between the MPC control modules and the district energy network.

After the initialization of the parameters, this procedure is carried out continuously with the LoTS and ShoTS different receding time horizon updates.

In particular, during real-time operation the LoTS module follows the timeline schematized in Figure 4. At each new day, the LoTS problem defined in Section 2.2 is written for the future period of the year (blue bar). The measurements from the real system are used to determine the actual operation and consumption, and to update the cumulated parameters (e.g. energy, fuel, and operating hours) of the previous period of the year (red bar). Once the solution has been found and the new long-term constraints have been defined, the horizon is diminished by one day and a new problem is solved.

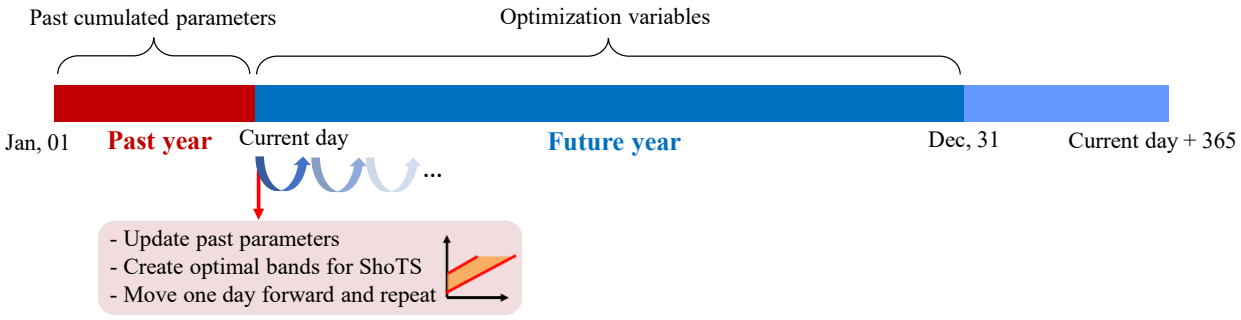

Figure 4. Timeline of the LoTS problem.

3. Application

The combined optimization algorithm is tested on a real case study by means of Model-in-the-Loop (MiL) simulations. The dynamics of the real system is accurately represented by its *digital twin* in a simulation environment, which serves as a virtual test bench. All relevant variables of the system can be quickly monitored to evaluate the performance of different control logics over an entire operating year. Hence, the proposed combined algorithm is applied and compared with the traditional way to manage the system.

3.1 Case study description

The case study is a hospital site located near the city of Ferrara, in northern Italy, with a yearly demand of heat, cold and electricity of 0.98, 0.83 and 1, respectively, when normalized with reference to the electrical demand for confidentiality reasons. The hospital is supplied by a district heating and a district cooling loop, while the thermal power station is a multi-energy system, illustrated in Figure 5, comprising the following energy conversion units:

- Four identical heat-only boilers (B) fed by natural gas, which supply the heating loop.
- A trigeneration plant consisting of an internal combustion engine in cogeneration mode (CHP) and an absorption chiller (ABS). The latter supplies cooling power to the cooling loop. The thermal power produced by the CHP can be sent to the heating loop, to ABS or dissipated into the environment.
- Four identical electric chillers (EC) which convert electrical power into cooling power for the cooling loop.

The electrical power balance is satisfied by means of a bidirectional exchange with the power grid: when the sum of hospital electrical demand and EC input is higher than the CHP power production, the remaining electrical power is purchased, while in the opposite case the surplus from the CHP is injected into the power grid. Both exchanges are subject to the limitations of the grid capacity.

The operating parameters of all plants are reported in Table 3. The hospital also has a steam demand met through steam generators located in a dedicated area, which do not interact with the rest of the system. This section is omitted from the analysis without hindering the generality of the approach. The maximum yearly operating time of the trigeneration unit is set to 8400 h. In particular, two maintenance periods of eight days each are scheduled for mid-April and mid-September.

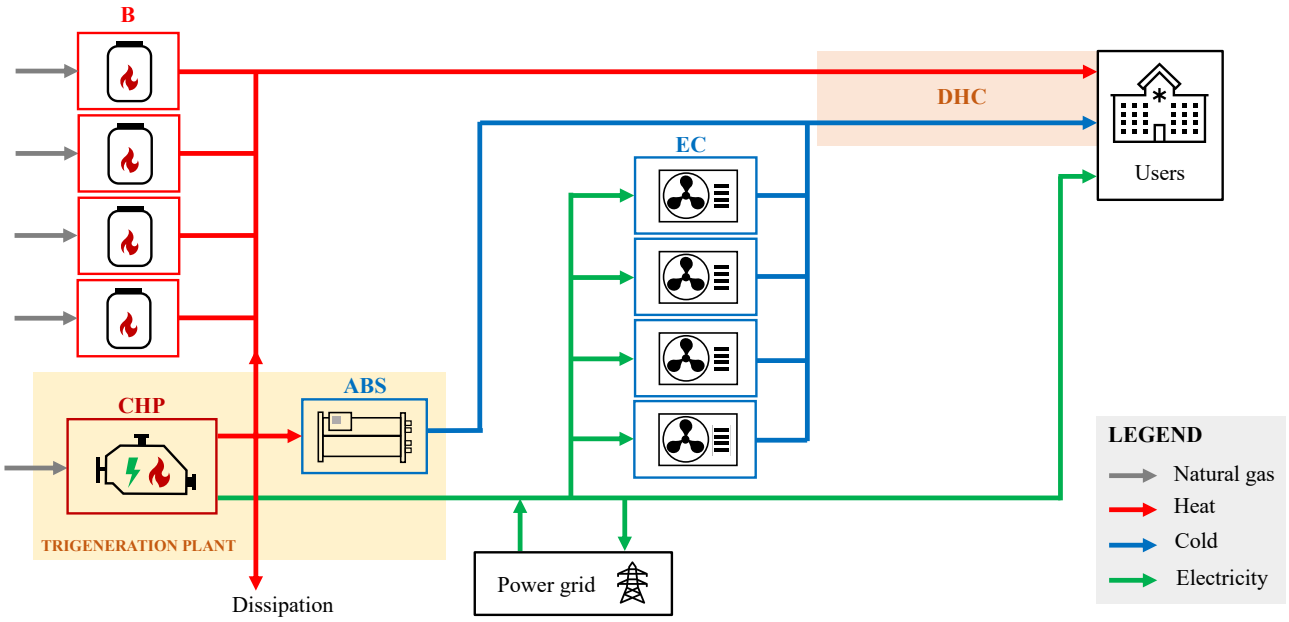

Figure 5. Schematic representation of the case study with the involved energy conversion units and energy vectors. B: boilers. CHP: Combined Heat and Power. ABS: absorption chiller. EC: electric chillers. DHC: District Heating and Cooling network.

Table 3. Main parameters of the thermal power station of the case study. The plant outputs are normalized with reference to the CHP electrical output for confidentiality reasons.

Parameter	B	CHP	ABS	EC
Number of units	4	1	1	4
Input	Natural gas	Natural gas	Heat	Electricity
Output	Heat	Electricity | Heat	Cold	Cold
Nominal output [-]	2.6	1 | 0.93	0.52	1.6
Nominal efficiency [-]	0.92	0.447 | 0.422	0.77	2
Min modulation [%]	5	50	20	5
Max operating hours [h]	-	8400	8400	-

The demands of heating, cooling and electrical power for three weeks of the year taken as representative examples of winter, mid-season and summer operation are reported in Figure 6, while the related market prices of electricity are shown in Figure 7. All demands are normalized with respect

to the maximum value reached by one of the energy vectors, due to confidentiality reasons. It is worth noting the high variability of the boundary conditions during the week but also throughout the year. Indeed, the combined MPC has to deal with these exogenous factors.

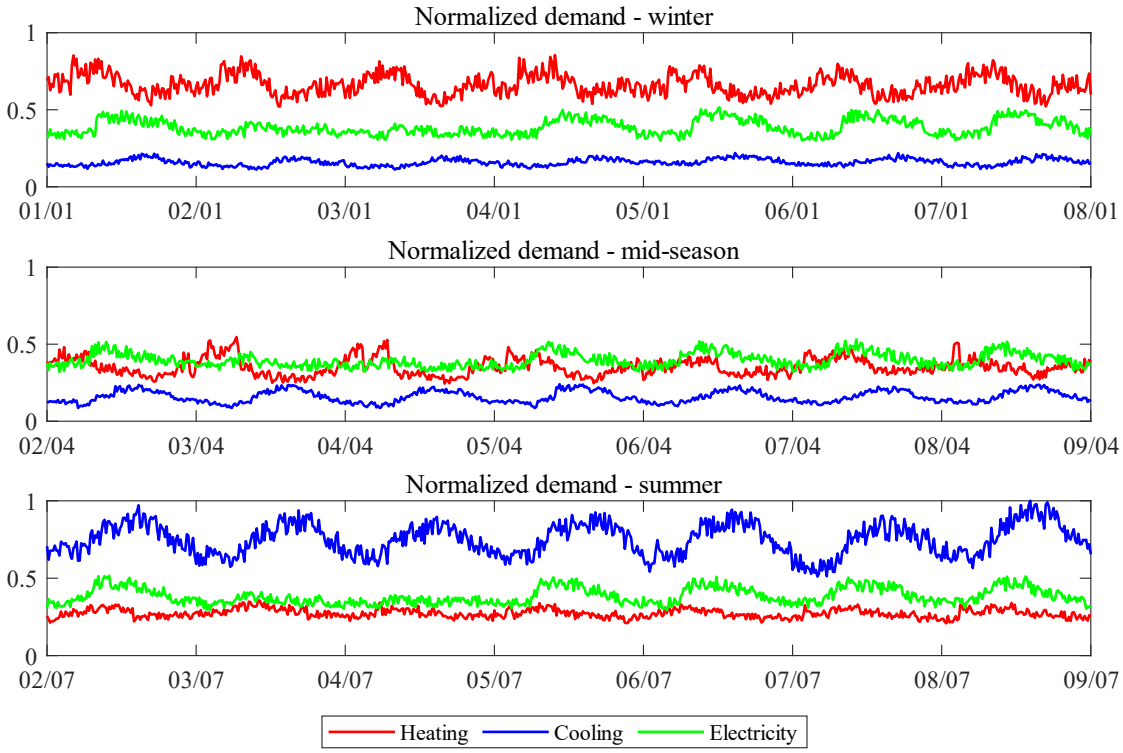

Figure 6. Normalized heating, cooling and electricity demand of the hospital case study of a winter, mid-season and summer week, with reference to the maximum value reached by one of the energy vectors.

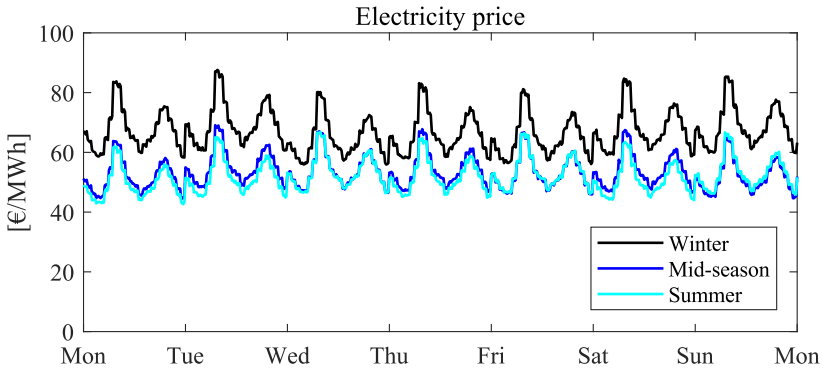

Figure 7. Market price of electricity for winter, mid-season and summer week.

3.2 Simulation setup

The system digital twin is built in the MATLAB®/Simulink® environment, by assembling the components from a custom library for energy systems simulation created by the authors and validated in several cases [42,43]. All blocks involve the physical flows of matter (e.g. water and fuel flows)

and energy as inputs and outputs. The energy conversion units can be controlled by varying such input flows. Their performance is determined by the operating parameters listed in the manufacturers' datasheets and generally involves a downgrading of the efficiency with the load and temperature conditions (e.g. in the case of CHP and EC). Both circuits for district heating and district cooling are composed by the pumps, expansion vessels, supply and return pipelines, primary heat exchangers (i.e. for transferring the thermal power produced by the plants to the circulating water) and user substation heat exchangers. The hydraulic and thermal dynamics of all elements are considered.

Benchmark control

The benchmark control logic represents the traditional way in which the energy systems of the real-world hospital are operated. The CHP is an electrical-load-following unit which, given the system size, results in a continuous operation at nominal load, except for the maintenance periods during which it is switched off, while ABS operates only during June, July and August. The water temperature in the supply pipeline of the district heating circuit is regulated as follows:

- if the temperature is lower than the set-point (i.e. 85 °C), the boilers are activated in cascade by a feedback loop;
- if the temperature is higher than the set-point, the boilers are switched off and part of the heat from the CHP, regulated by a feedback loop, is dissipated.

The supply temperature of the district cooling circuit is controlled similarly:

- if it is lower than the set-point (i.e. 6 °C), all units producing cooling power are switched off;
- if it is higher than the set-point, the EC are activated in sequence to provide sufficient cooling power until the desired value is reached.

There are additional low-level controllers for the system actuators. In particular, a feedback loop varies the pump rotational speed in order to match the reference temperature difference between supply and return in the user substation (i.e. 25 °C and 6 °C for the heating and cooling circuits, respectively).

MPC control

Conversely, the MPC control logic gives the set-points for the operation of CHP and ABS, as well as the activation signals of the boilers and EC. These data correspond to the first time-step of the optimal sequence calculated by ShoTS in accordance with LoTS constraints. However, the boilers and EC are still regulated in series as in the benchmark case, in order to ensure compliance with the desired operating parameters of the district heating and cooling network. In addition, the actual demand of the energy vectors implemented in the digital twin is different from the forecast fed to the ShoTS and LoTS modules. Thus, for these reasons, the actual operation registered in the system digital twin differs from that predicted by the combined MPC. At every ShoTS time-step, the state of the plants and actual energy and fuel consumption are acquired and sent to the MPC algorithms, which update their parameters and solutions according to the flowchart in Figure 3. This MiL procedure, summarized in Figure 8, is carried out continuously for the entire operating year.

The strategy to regulate the low-level actuators is the same as the benchmark case.

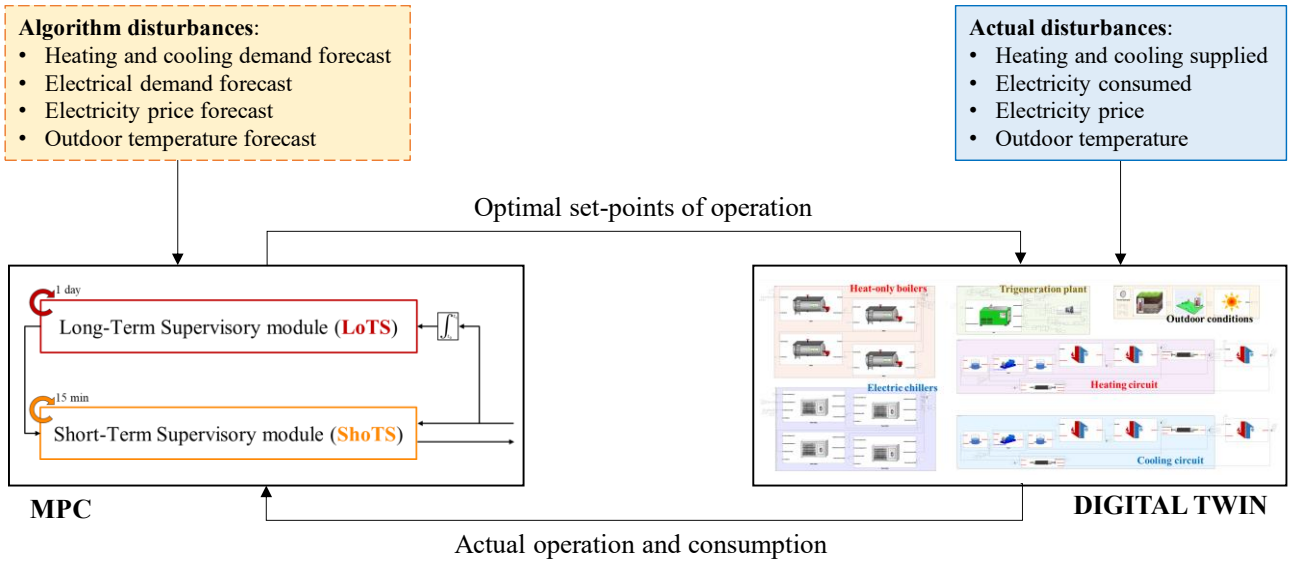

Figure 8. Model-in-the-Loop simulation setup. It is highlighted that the forecast disturbances sent to the MPC are different from the actual disturbances, as in a real-world case.

4. Results and discussion

This section presents the results of the simulation case study described in Section 3. The comparative results over a whole year of operation with the benchmark control strategy and with the combined MPC controller are reported in Table 4. The total operating cost of the system management is calculated as the LoTS cost function: sum of the fuel cost and electricity purchased from the grid decreased by the revenues from the sale of surplus electricity (considering the actual market price hour by hour) and the energy efficiency certificates awarded at the end of the year. The carbon dioxide emissions related to system operation are calculated by assuming emission factors of 2.16 kg_{CO2}/Nm^3 and 445.5 kg_{CO2}/MWh for natural gas [44] and electricity from the grid [45], respectively. As for natural gas, a fixed price of 0.23 €/Nm^3 has been considered.

Table 4. Comparative results for the whole-year simulations with different control strategies.

Result	MPC vs. benchmark
Operating cost	-9.7%
Primary energy consumption	-0.05%
Fuel consumption	+9.9%
CHP overall efficiency	+4.9%
CHP primary energy saving	+12.7%
CHP energy efficiency certificates	+9.8%
Dissipated heat	-99.8%
Electricity sale to grid	+625%
Electricity purchase from grid	-27.4%
Carbon dioxide emissions	+0.97%

It can be noted that the MPC accomplishes the goal of reducing the total operating cost of system management over the whole year. The performance of the CHP plant is significantly enhanced compared to the benchmark control, since both the overall efficiency (i.e. the ratio between the sum of the useful electrical and thermal energy produced and the fuel energy input) and total primary energy saving of the unit increase. In particular, the CHP is operated in order to reduce heat dissipation as much as possible (-99.8%) and to increase the revenues from incentives on high efficiency cogeneration (+9.8%). This is achieved thanks to the LoTS cost function, which is able to maximize the energy efficiency certificates (evaluated on the basis of the whole-year operation) and

to transmit information on this optimal yearly operation to the ShoTS module so that it is converted into real-time control action.

Together with a 9.7% reduction in the operating cost, the global purchase of electricity is reduced by more than 27% in the MPC case, showing that it is preferable to exploit the production from the available units in the thermal power station and reduce dependency on the power grid. This comes together with an increase in fuel consumption by around 10% but also with a slight decrease in primary energy consumption, calculated by considering the net electricity between that purchased and that injected into the grid (an average conversion efficiency of the Italian national grid of 0.46 is assumed). Finally, carbon dioxide emissions are slightly higher in the MPC operation. However, it is important to recall that the cost functions of both long-term and short-term optimization algorithms do not include the environmental performance of the system. A different goal or a multi-objective optimization strategy [16] may lead to a different output.

Figure 9 shows that the described results are due to the different shares of energy vector production and consumption. In particular, the absorption chiller is used to a greater extent in the MPC operation (i.e. around 47% of total cold production). This is because MPC makes it possible to calculate the cost-effectiveness of the absorption chiller and electric chiller share more precisely also when the cold demand is relatively low (winter and mid-seasons), compared to the benchmark case in which a fixed operation schedule is defined.

Furthermore, Figure 10 confirms the lower share of electricity from the grid in the total primary energy in favor of higher fuel exploitation. Since this was obtained with a conservative natural gas price, a different value or a variable price may give a difference result. It is also remarked that the heat dissipation is reduced to a value lower than 1%.

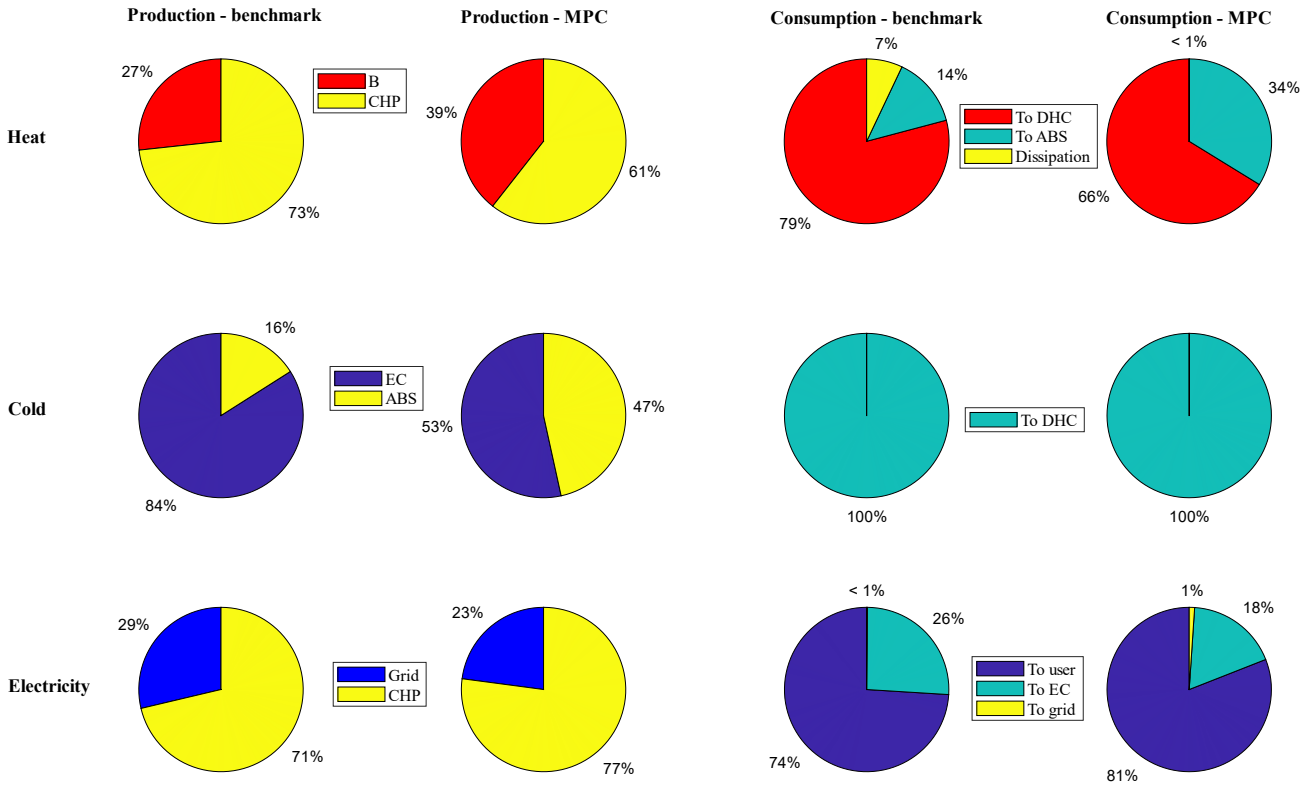

Figure 9. Share of total energy production and consumption in the benchmark and MPC operation (heat, cold and electricity).

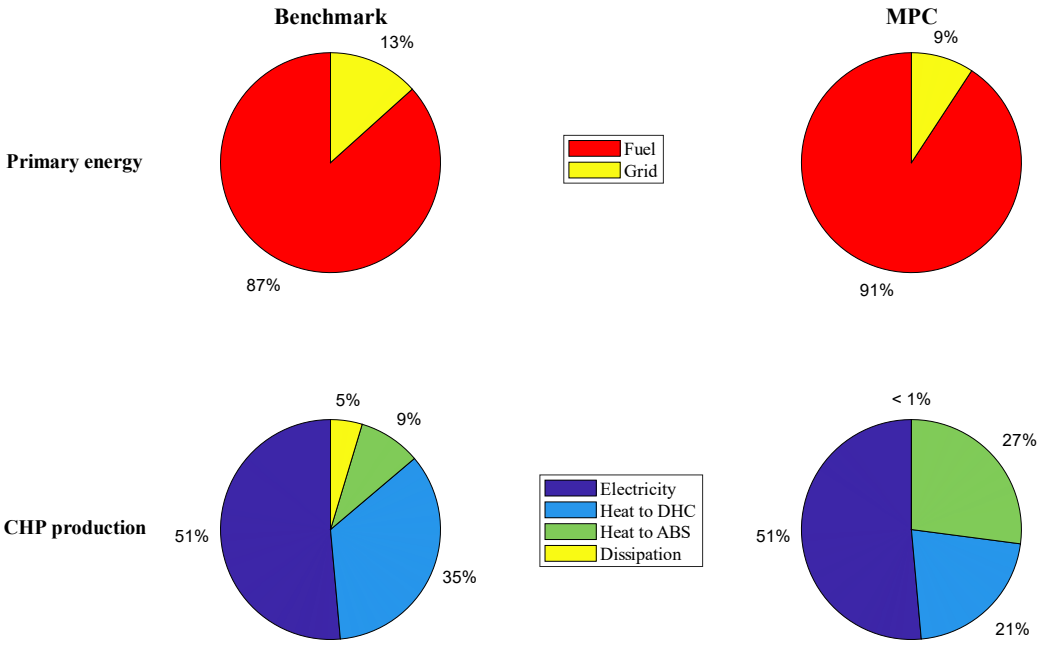

Figure 10. Share of primary energy and CHP production.

The share of the production and consumption of the different forms of energy is further detailed in Figure 11, where the monthly values are reported and compared. All values are normalized with respect to the maximum of each chart, in order to show the variation in each contribution over the year. It can be noted that the MPC operation favors heat production in colder months, in order to adopt the absorption chiller. Furthermore, it avoids a significant amount of heat dissipation in particular in May, September and November, when the user heat demand is lower and the CHP is modulated more effectively. As for cold production, the trigeneration is controlled in such a way that the exploitation of electric chillers is almost avoided in winter.

In agreement with previous studies from the authors [38], the presented optimal control strategy displays the best performance during mid-seasons, when the external conditions are generally subject to greater variations, which can be effectively forecast and dealt with by the MPC. The hourly shares of energy production and consumption during a representative spring day (i.e. May, 10) are illustrated in Figure 12, in order to underline these effects.

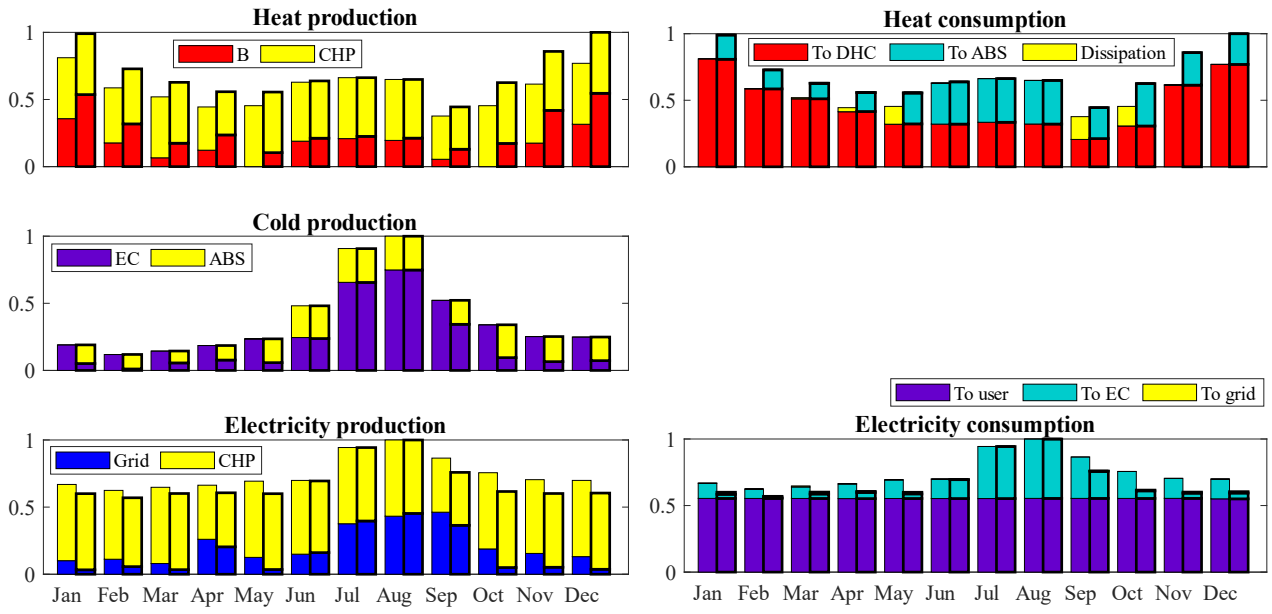

(a) (b)

Figure 11. Share of (a) monthly energy production and (b) monthly energy consumption in the benchmark and MPC operation (heat, cold and electricity). The bars highlighted in bold are related to the MPC operation. All values are normalized with respect to the maximum of each chart. The share of cold consumption is omitted as it is trivial.

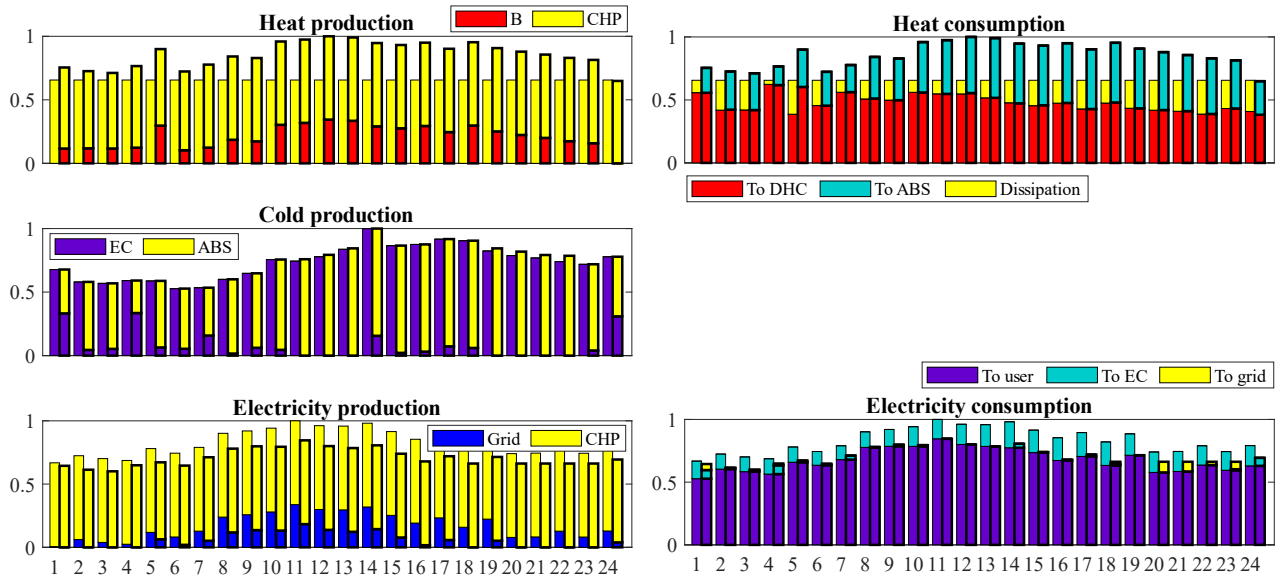

Figure 12. Share of (a) hourly energy production and (b) hourly energy consumption in the benchmark and MPC operation during a May day (May, 10). The bars highlighted in bold are related to the MPC operation. All values are normalized with respect to the maximum of each chart. The share of cold consumption is omitted as it is trivial.

It is worth remarking that these data are not a result of the perfect forecast either of the ShoTS or the LoTS modules, but they are related to the actual operation of the controlled system, which is subject to exogenous factors with a certain degree of uncertainty, as in reality.

Figure 13 shows the computational feasibility of the method in real-time control. Each bar indicates the absolute frequency of the solution time of the ShoTS problem. The distribution is highly gathered toward solution times lower than 5 seconds, with just a few occurrences higher than 10 seconds. This is considered acceptable for the supervisory control of a multi-energy system. Furthermore, it is worth pointing out that the solution of each one of the MPC modules contains the optimal control sequence of the next prediction horizon, which is saved in the memory. If the problem does not converge or takes an infeasible computational time at a certain time-step k, it is possible to rely on the solution obtained at time-step k-1 for time-step k. This backup configuration may lead to sub-optimal operation locally, but it is regarded as a feasible option to deal with potential algorithm failures in real-time control.

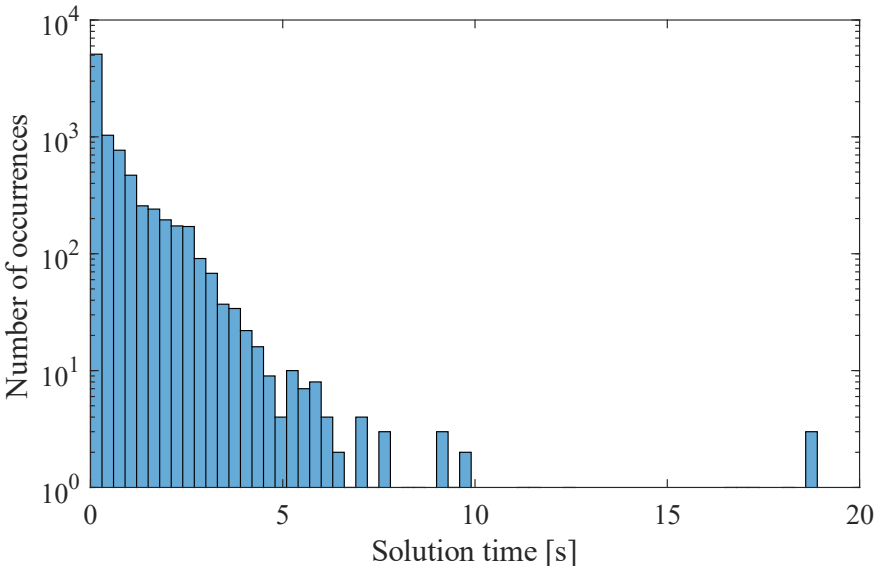

Figure 13. Distribution of computational time in the ShoTS calculation over the whole year simulation.

The calculation times of all LoTS iterations during all days of the simulated year are instead shown in Figure 14. As expected, the solution time decreases over the year, as the consequent decreasing prediction horizon up to the end of the year makes the problem dimension smaller. In any case, the computational effort is very low even during the first days for a module that has to be updated every day, because LoTS solves a Linear Programming, which is faster than an MILP. This allows several upgrading options to be considered for the LoTS problem, e.g. a prediction horizon of 365 days for all yearly iterations, or even scheduling maintenance during optimal time periods as part of the optimization problem.

Overall, the applicability of the proposed tool in autonomous real-time control of multi-source district energy networks has been assessed. Thus, it may also be used to automatically control (i) systems bound by specific contract limitations on electricity purchase/injection from/into the grid and on fuel purchase, and (ii) systems with long-term storage.

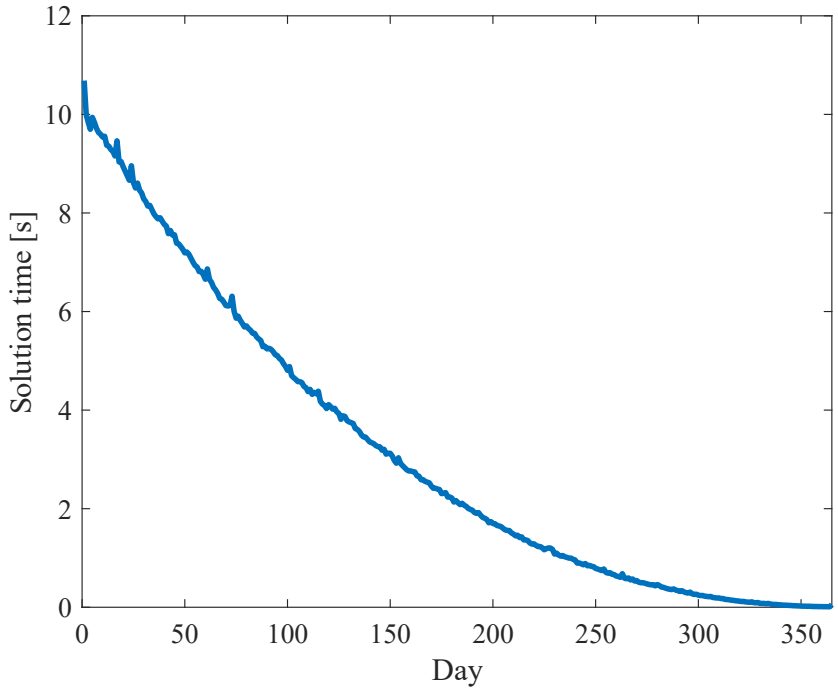

Figure 14. Computational time of the LoTS calculation on all days of the year.

Finally, this research is on the same path as the global framework demonstrated in [42] for the development of smart controllers for integrated energy systems. After the setup and verification of the algorithm in a simulation environment, this is currently in the phases of (i) implementation in the real-world hospital case study and (ii) experimental investigation. The presented application serves as a baseline for the future experimental study of the hospital site. Data collection campaigns from sensors installed in the real system will be carried out in order to obtain a complete overview of the new MPC performance.

Due to the fact that the algorithm operates as a supervisory controller generating optimal system set-points (which are maintained by existing low-level controllers within the plants), the real-world implementation is straightforward and does not require changes to the system layout. Indeed, the algorithm is able to (i) run automatically on a computer or control toolbox within the control room and (ii) pass the calculated set-points to the plant through standard communication protocols.

Together with the real field tests, the future developments of the project will focus on the investigation and further assessment of the combined algorithm properties and performance in more complex networks, such as:

- systems with different types of storage, e.g. both short-term and seasonal storage;
- systems with a higher penetration of fluctuating renewable energy sources, with the integration of power-to-gas technologies to serve as storage;
- renewable energy communities.

5. Conclusions

This work presented an original combined optimization algorithm for optimally managing multi-source energy systems. The optimization was divided into three coordinated modules, each responsible for part of the problem: different multi-agent distribution modules minimized the energy supplied to the branches of the distribution network, while two combined supervisory modules performed smart control of the production site. In particular, the long-term supervisory algorithm solved a whole-year scheduling problem considering factors such as year-based incentives and contracts. It also determined the long-term constraints for the short-term supervisory algorithm, which calculated in real-time the optimal control inputs over a short prediction horizon. Each of these modules was a Model Predictive Control (MPC) that was periodically updated (every time-step) with new information deriving from the controlled system monitoring and disturbance forecast, in order to improve its robustness with respect to exogenous factors.

The original approach was tested on a hospital case study, comprising a multi-energy thermal power station with boilers, electric chillers, a Combined Heat and Power unit (CHP) and an absorption chiller (ABS) for the production of heating, cooling and electrical power, as well as two district heating and cooling loops that supply energy to the hospital buildings. The proposed combined algorithm was used to manage in real-time the system digital twin in a simulation environment, and the results were compared to those obtained with a traditional benchmark control. The MPC approach led to a 9.7% reduction in yearly operating cost and to slightly lower global primary energy consumption. The operation of the CHP unit was significantly enhanced to reduce heat dissipation as

much as possible and to use such excess heat as input to ABS. Moreover, the CHP overall efficiency and primary energy saving increased by 4.9% and 12.7%, respectively, leading to a greater financial remuneration of high efficiency cogeneration through incentives. In addition, the system dependency on the power grid was reduced, as there was more than a 24% decrease in the total amount of electricity purchased.

These outcomes were made possible by binding the short-term optimization module through long-term constraints deriving from the whole-year optimization module, leading to effective integration not only of different energy vectors but also of different time scales in smart control. The modular and generic nature of the combined algorithm makes it applicable to several types of multi-energy systems, including the contribution of power-to-gas technologies, long-term storage and renewable energy sources. These features will be further investigated in future upgrades of this research, together with its experimental verification in the real-world case study.

Acknowledgements

This work was supported by the "DISTRHEAT – Digital Intelligent and Scalable conTrol for Renewables in HEAting neTworks" project, which received funding in the framework of the joint programming initiative ERA-Net Smart Energy Systems' focus initiative Integrated, Regional Energy Systems, with support from the European Union's Horizon 2020 research and innovation programme under grant agreement No 775970.

References

[1] Bernath C, Deac G, Sensfuß F. Impact of sector coupling on the market value of renewable energies – A model-based scenario analysis. Appl Energy 2021;281. https://doi.org/10.1016/j.apenergy.2020.115985.

[2] Gea-Bermúdez J, Jensen IG, Münster M, Koivisto M, Kirkerud JG, Chen Y kuang, et al. The role of sector coupling in the green transition: A least-cost energy system development in Northern-central Europe towards 2050. Appl Energy 2021;289:116685. https://doi.org/10.1016/j.apenergy.2021.116685.

[3] Fridgen G, Keller R, Körner MF, Schöpf M. A holistic view on sector coupling. Energy Policy 2020;147. https://doi.org/10.1016/j.enpol.2020.111913.

[4] Mancarella P. MES (multi-energy systems): An overview of concepts and evaluation models. Energy 2014;65:1–17. https://doi.org/10.1016/j.energy.2013.10.041.

[5] Guelpa E, Bischi A, Verda V, Chertkov M, Lund H. Towards future infrastructures for sustainable multi-energy systems: A review. Energy 2019;184:2–21. https://doi.org/10.1016/j.energy.2019.05.057.

[6] Møller Sneum D. Barriers to flexibility in the district energy-electricity system interface – A taxonomy. Renew Sustain Energy Rev 2021;145. https://doi.org/10.1016/j.rser.2021.111007.

[7] Bitar E, Khargonekar PP, Poolla K. Systems and control opportunities in the integration of renewable energy into the Smart Grid. vol. 44. IFAC; 2011. https://doi.org/10.3182/20110828-6-IT-1002.01244.

[8] Zhao X, Zheng W, Hou Z, Chen H, Xu G, Liu W, et al. Economic dispatch of multi-energy system considering seasonal variation based on hybrid operation strategy. Energy 2022;238:121733. https://doi.org/10.1016/j.energy.2021.121733.

[9] Lund H, Duic N, Østergaard PA, Mathiesen BV. Future district heating systems and technologies: On the role of smart energy systems and 4th generation district heating. Energy 2018;165:614–9. https://doi.org/10.1016/j.energy.2018.09.115.

[10] Lund H, Østergaard PA, Connolly D, Mathiesen BV. Smart energy and smart energy systems. Energy 2017;137:556–65. https://doi.org/10.1016/j.energy.2017.05.123.

[11] Morales-España G, Latorre JM, Ramos A. Tight and compact MILP formulation for the thermal unit commitment problem. IEEE Trans Power Syst 2013;28:4897–908. https://doi.org/10.1109/TPWRS.2013.2251373.

[12] Bischi A, Taccari L, Martelli E, Amaldi E, Manzolini G, Silva P, et al. A detailed MILP optimization model for combined cooling, heat and power system operation planning. Energy 2014;74:12–26. https://doi.org/10.1016/j.energy.2014.02.042.

[13] Moretti L, Martelli E, Manzolini G. An efficient robust optimization model for the unit commitment and dispatch of multi-energy systems and microgrids. Appl Energy 2020;261:113859. https://doi.org/10.1016/j.apenergy.2019.113859.

[14] Wirtz M, Neumaier L, Remmen P, Müller D. Temperature control in 5th generation district heating and cooling networks: An MILP-based operation optimization. Appl Energy 2021;288:116608. https://doi.org/10.1016/j.apenergy.2021.116608.

[15] Ghilardi LMP, Castelli AF, Moretti L, Morini M, Martelli E. Co-optimization of multi-energy system operation, district heating/cooling network and thermal comfort management for buildings. Appl Energy 2021;302:117480. https://doi.org/10.1016/j.apenergy.2021.117480.

[16] Capone M, Guelpa E, Verda V. Multi-objective optimization of district energy systems with demand response. Energy 2021;227:120472. https://doi.org/10.1016/j.energy.2021.120472.

[17] Gambarotta A, Morini M, Pompini N, Spina PR. Optimization of load allocation strategy of a multi-source energy system by means of dynamic programming. Energy Procedia 2015;81:30–9. https://doi.org/10.1016/j.egypro.2015.12.056.

[18] Urbanucci L. Limits and potentials of Mixed Integer Linear Programming methods for optimization of polygeneration energy systems. Energy Procedia 2018;148:1199–205. https://doi.org/10.1016/j.egypro.2018.08.021.

[19] Bragin MA, Luh PB, Yan B, Sun X. A scalable solution methodology for mixed-integer linear

programming problems arising in automation. IEEE Trans Autom Sci Eng 2019;16:531–41. https://doi.org/10.1109/TASE.2018.2835298.

[20] Moustakidis S, Meintanis I, Halikias G, Karcanias N. An innovative control framework for district heating systems: Conceptualisation and preliminary results. Resources 2019;8:1–15. https://doi.org/10.3390/resources8010027.

[21] Mugnini A, Coccia G, Polonara F, Arteconi A. Energy flexibility as additional energy source in multi-energy systems with district cooling. Energies 2021;14. https://doi.org/10.3390/en14020519.

[22] Banta L, Rossi I, Traverso A, Traverso AN. Advanced control of a real smart polygeneration microgrid. Energy Procedia 2014;61:274–7. https://doi.org/10.1016/j.egypro.2014.11.1106.

[23] Moser A, Muschick D, Gölles M, Nageler P, Schranzhofer H, Mach T, et al. A MILP-based modular energy management system for urban multi-energy systems: Performance and sensitivity analysis. Appl Energy 2020;261:114342. https://doi.org/10.1016/j.apenergy.2019.114342.

[24] Jiao F, Zou Y, Zhang X, Zhang B. Online optimal dispatch based on combined robust and stochastic model predictive control for a microgrid including EV charging station. Energy 2022;247:123220. https://doi.org/10.1016/j.energy.2022.123220.

[25] Lyden A, Tuohy PG. Planning level sizing of heat pumps and hot water tanks incorporating model predictive control and future electricity tariffs. Energy 2022;238:121731. https://doi.org/10.1016/j.energy.2021.121731.

[26] Bahlawan H, Losi E, Manservigi L, Morini M, Pinelli M, Spina PR, et al. Optimal design and energy management of a renewable energy plant with seasonal energy storage. E3S Web Conf 2021;238. https://doi.org/10.1051/e3sconf/202123802002.

[27] Gabrielli P, Fürer F, Mavromatidis G, Mazzotti M. Robust and optimal design of multi-energy systems with seasonal storage through uncertainty analysis. Appl Energy 2019;238:1192–210. https://doi.org/10.1016/j.apenergy.2019.01.064.

[28] Bohlayer M, Bürger A, Fleschutz M, Braun M, Zöttl G. Multi-period investment pathways - Modeling approaches to design distributed energy systems under uncertainty. Appl Energy 2021;285:116368. https://doi.org/10.1016/j.apenergy.2020.116368.

[29] Fazlollahi S, Bungener SL, Mandel P, Becker G, Maréchal F. Multi-objectives, multi-period optimization of district energy systems: I. Selection of typical operating periods. Comput Chem Eng 2014;65:54–66. https://doi.org/10.1016/j.compchemeng.2014.03.005.

[30] Bartolucci L, Cordiner S, Mulone V, Pasquale S, Sbarra A. Design and management strategies for low emission building-scale Multi Energy Systems. Energy 2022;239:122160. https://doi.org/10.1016/j.energy.2021.122160.

[31] Bischi A, Taccari L, Martelli E, Amaldi E, Manzolini G, Silva P, et al. A rolling-horizon optimization algorithm for the long term operational scheduling of cogeneration systems. Energy 2019;184:73–90. https://doi.org/10.1016/j.energy.2017.12.022.

[32] Li P, Guo T, Abeysekera M, Wu J, Han Z, Wang Z, et al. Intraday multi-objective hierarchical coordinated operation of a multi-energy system. Energy 2021;228:120528. https://doi.org/10.1016/j.energy.2021.120528.

[33] Chiam Z, Easwaran A, Mouquet D, Fazlollahi S, Millás J V. A hierarchical framework for holistic optimization of the operations of district cooling systems. Appl Energy 2019;239:23–40. https://doi.org/10.1016/j.apenergy.2019.01.134.

[34] Bornand B, Girardin L, Belfiore F, Robineau JL, Bottallo S, Maréchal F. Investment Planning Methodology for Complex Urban Energy Systems Applied to a Hospital Site. Front Energy Res 2020;8:1–18. https://doi.org/10.3389/fenrg.2020.537973.

[35] Naughton J, Wang H, Riaz S, Cantoni M, Mancarella P. Optimization of multi-energy virtual power plants for providing multiple market and local network services. Electr Power Syst Res 2020;189:106775. https://doi.org/10.1016/j.epsr.2020.106775.

[36] Naughton J, Wang H, Cantoni M, Mancarella P. Co-Optimizing Virtual Power Plant Services under Uncertainty: A Robust Scheduling and Receding Horizon Dispatch Approach. IEEE

Trans Power Syst 2021;36:3960–72. https://doi.org/10.1109/TPWRS.2021.3062582.

[37] Li P, Wang Z, Wang J, Guo T, Yin Y. A multi-time-space scale optimal operation strategy for a distributed integrated energy system. Appl Energy 2021;289:116698. https://doi.org/10.1016/j.apenergy.2021.116698.

[38] Saletti C, Gambarotta A, Morini M. Development, analysis and application of a predictive controller to a small-scale district heating system. Appl Therm Eng 2020;165:114558. https://doi.org/10.1016/j.applthermaleng.2019.114558.

[39] Mansoor M, Stadler M, Zellinger M, Lichtenegger K, Auer H, Cosic A. Optimal planning of thermal energy systems in a microgrid with seasonal storage and piecewise affine cost functions. Energy 2021;215:119095. https://doi.org/10.1016/j.energy.2020.119095.

[40] Carrión M, Arroyo JM. A computationally efficient mixed-integer linear formulation for the thermal unit commitment problem. IEEE Trans Power Syst 2006;21:1371–8. https://doi.org/10.1109/TPWRS.2006.876672.

[41] Alemany J, Magnago F, Moitre D, Pinto H. Symmetry issues in mixed integer programming based Unit Commitment. Int J Electr Power Energy Syst 2014;54:86–90. https://doi.org/10.1016/j.ijepes.2013.06.034.

[42] De Lorenzi A, Gambarotta A, Morini M, Rossi M, Saletti C. Setup and testing of smart controllers for small-scale district heating networks: An integrated framework. Energy 2020;205:118054. https://doi.org/10.1016/j.energy.2020.118054.

[43] Ancona MA, Branchini L, De Lorenzi A, De Pascale A, Gambarotta A, Melino F, et al. Application of different modeling approaches to a district heating network. AIP Conf Proc 2019;2191. https://doi.org/10.1063/1.5138742.

[44] OCCC (Catalan Office for Climate Change). Practical guide for calculating Greenhose Gas (GHG) emissions 2019:125.

[45] ISPRA Istituto Superiore per la Protezione e la Ricerca Ambientale. Fattori di emissione atmosferica di gas a effetto serra nel settore elettrico nazionale e nei principali Paesi Europei.

2019.

Nomenclature

C	daily average cost [€/MWh]
c	cost [€/MWh] or [€/Nm^3]
D	number of days of ShoTS prediction horizon [-]
E	energy [MWh]
LHV	lower heating value [kJ kg^{-1}]
M	maximum auxiliary variable [MWh]
m	minimum auxiliary variable [MWh]
N	number of time-steps [-]
N_d	number of days of LoTS prediction horizon [-]
OH	operating hours [h]
P	power [kW]
SU	start-up additional power [kW]
t	time [s]
α	coefficient of unit performance curve [-]
β	coefficient of unit performance curve [kW]
γ	stand-by switch (binary) [-]
δ	on-off switch (binary) [-]
ε	daily availability variable [-]
η	efficiency [-]

Superscripts

c	cooling
el	electricity
f	fuel
h	heating
I	related to overall efficiency

Subscripts

bg	bought from power grid
dem	demand
diss	dissipation
down	related to a decrease in power input
el	electrical
f	fuel
h	thermal
in	input
inc	incentive
j	generic unit
k	generic time-step
l	generic energy vector
max	maximum
min	minimum
output	output
past	related to the previous period of the year
ref	reference
sby	related to stand-by mode

sg	sold to power grid
SU	related to start-up
up	related to an increase in power input
y	yearly

Acronyms

ABS	Absorption chiller
B	Boiler
CHP	Combined Heat and Power
DHC	District Heating and Cooling
EC	Electric chiller
LoTS	Long-Term Supervisory module
MiL	Model-in-the-Loop
MILP	Mixed Integer Linear Programming
MPC	Model Predictive Control
PES	Primary Energy Saving
ShoTS	Short-Term Supervisory module